Supplementary Information

Lithium Storage Properties of In-situ Li$_2$FeSiO$_4$ and LiFeBO$_3$ Nanocomposites as

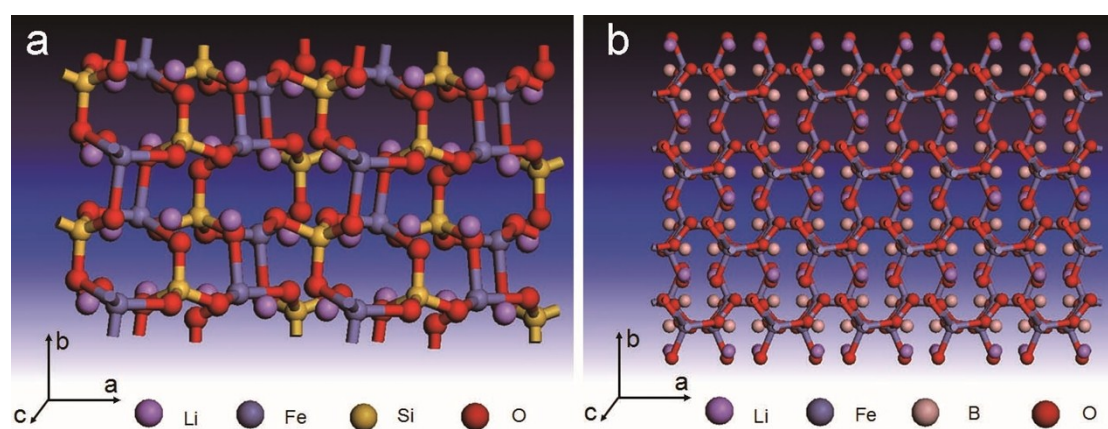**Advanced Cathode Materials for Lithium Ion Batteries**

Lin Hu, Jinlong Yang, Ibrahim Saana Amiinu, Xiaochun Kang, Wei Zhang and

Shichun Mu[*]

State Key Laboratory of Advanced Technology for Materials Synthesis and

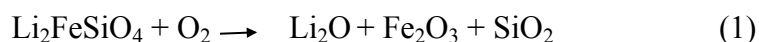Progressing, Wuhan University of Technology, Wuhan，430070

E-mail: msc@whut.edu.cn

Figure S1. The crystal structure of Li$_2$FeSiO$_4$ (a) and LiFeBO$_3$ (b) viewed along the c-axis.

TG analyses

In the oxygen atmosphere, the reaction of the pure LFS is as following (1): suffering from a weight increase from 100 wt. % to 105 wt. %.

$$Li_2FeSiO_4 + O_2 \longrightarrow Li_2O + Fe_2O_3 + SiO_2 \qquad (1)$$

For LFS/C and 0.92LFS·0.08LFB/C composites, the final residues have the analogous composition with the pure LFS sample after 900℃, as following (2):

$$Li_2FeSiO_4/C + O_2 \longrightarrow Li_2O + Fe_2O_3 + SiO_2 + CO_2\uparrow \qquad (2)$$
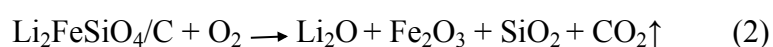
Because of the solid product of LFS/C after reaction with LFS the same, the weight content of the LFS content in the LFS/C is the final percentage weight/105 wt. %, so the carbon content (100 % - (the final percentage weight/105 wt. %)) in the LFS/C and 0.92LFS·0.08LFB/C composites is 11.66 % and 11.59 %, respectively. In our experiments, TGA was conducted in air (oxygen) over a temperature range of 25–900 oC. In **Figure S2**, the increased weight at ~80 ℃ in both samples is probably due to slight oxidation of Fe^{2+}. The increased weight around 300 ℃ could be caused by a large number of LFS oxidation which has not been identified, the reaction as following (3):

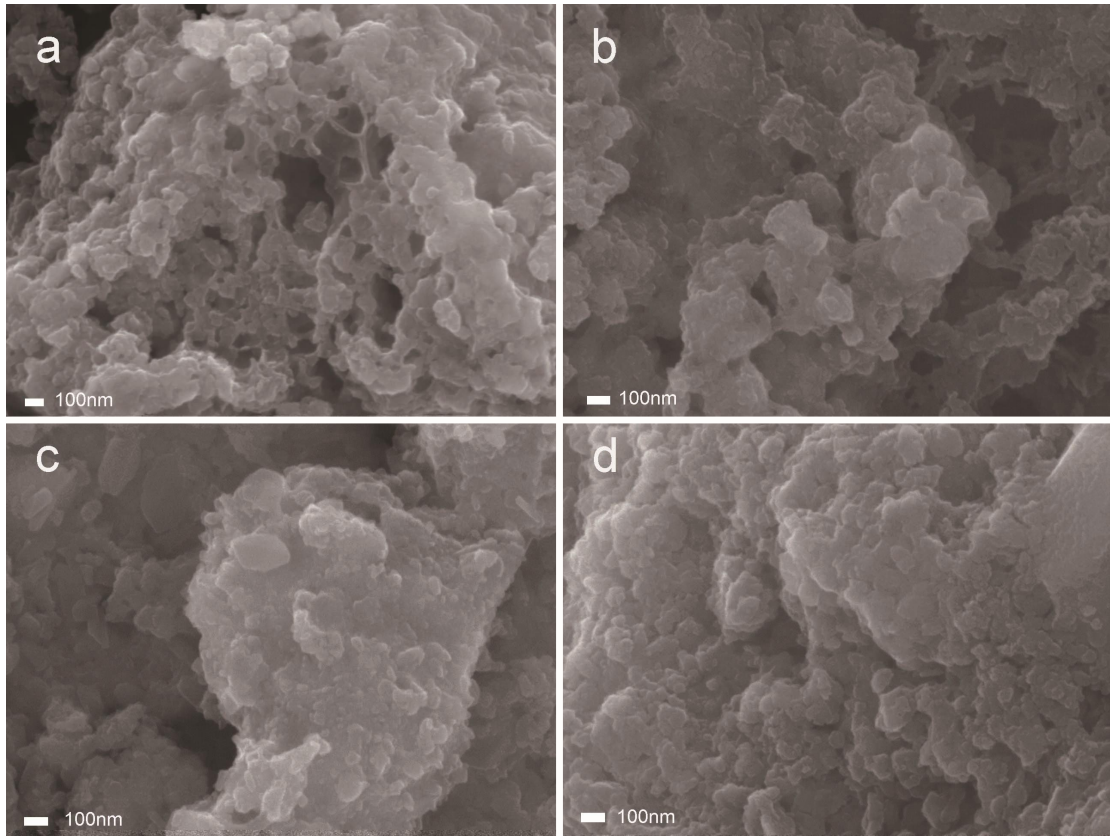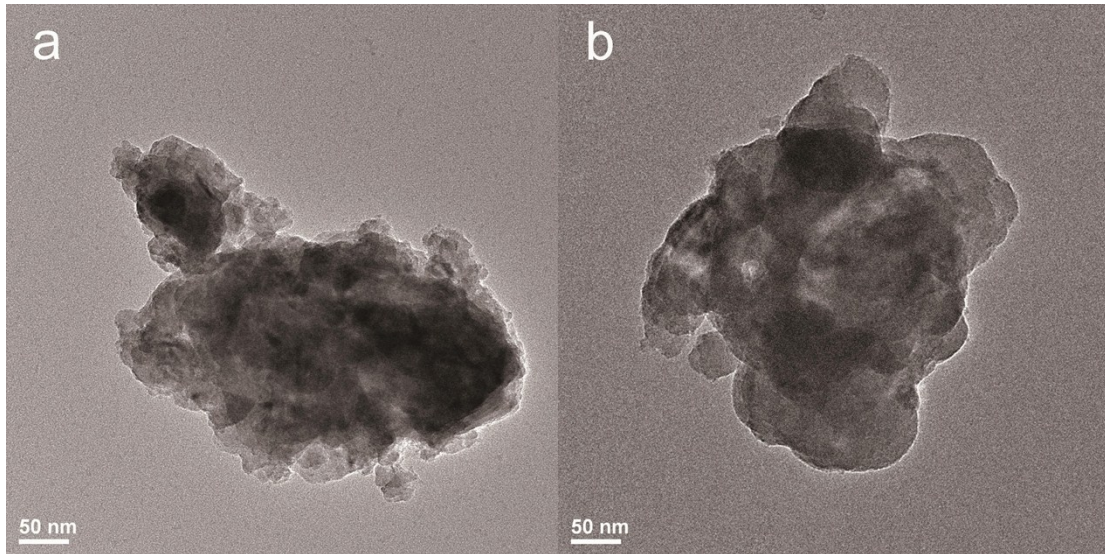$$Li_2FeSiO_4/C + O_2 \longrightarrow Li_2CO_3 + LiFeSiO_4 \qquad (3)$$
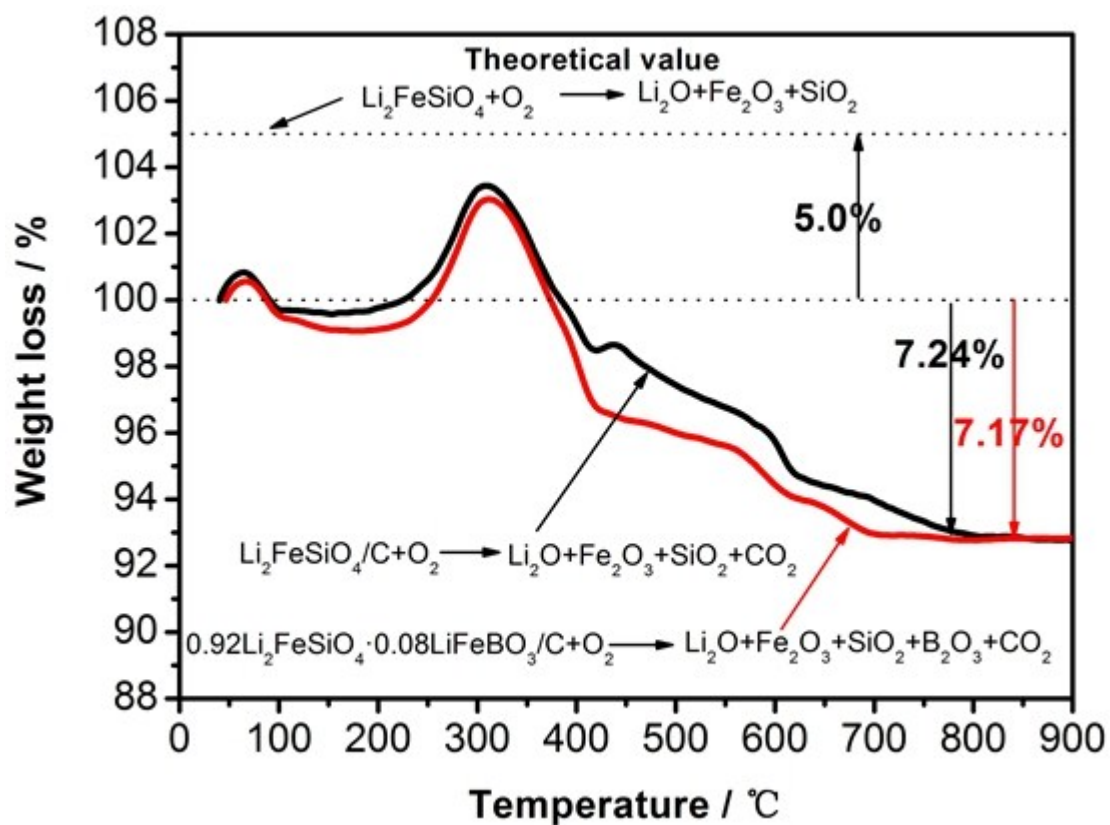
Figure S2. Thermogravimetric analysis (TG) curves of (1-x)LFS·xLFB/C composites with x=0 and 0.08.
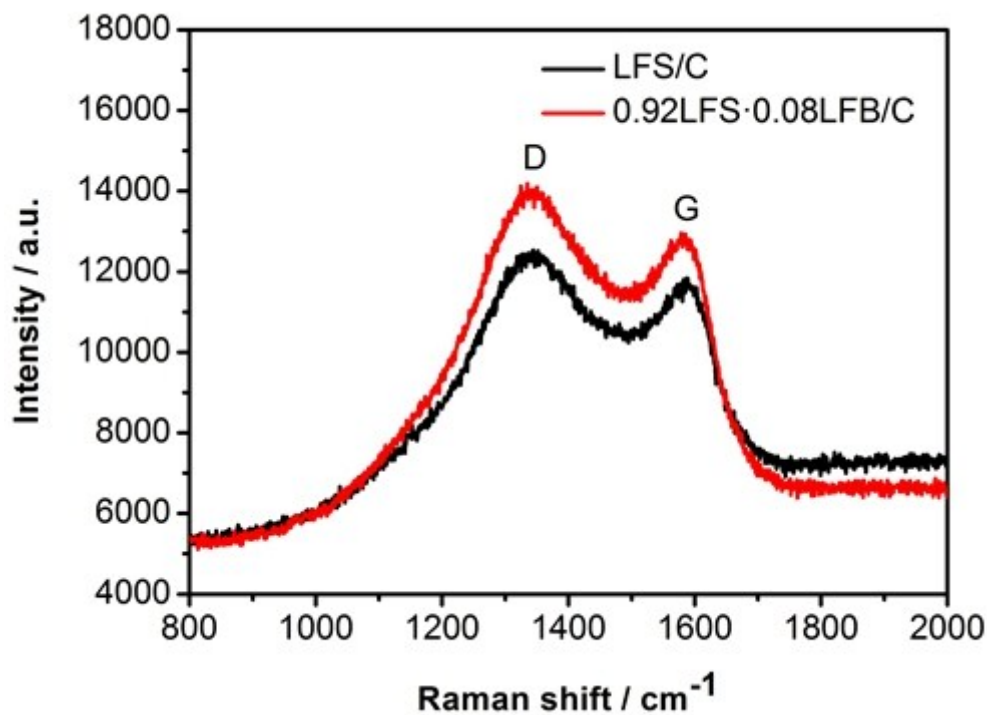
Figure S3. Raman spectra of LFS/C and 0.92LFS·0.08LFB/C.
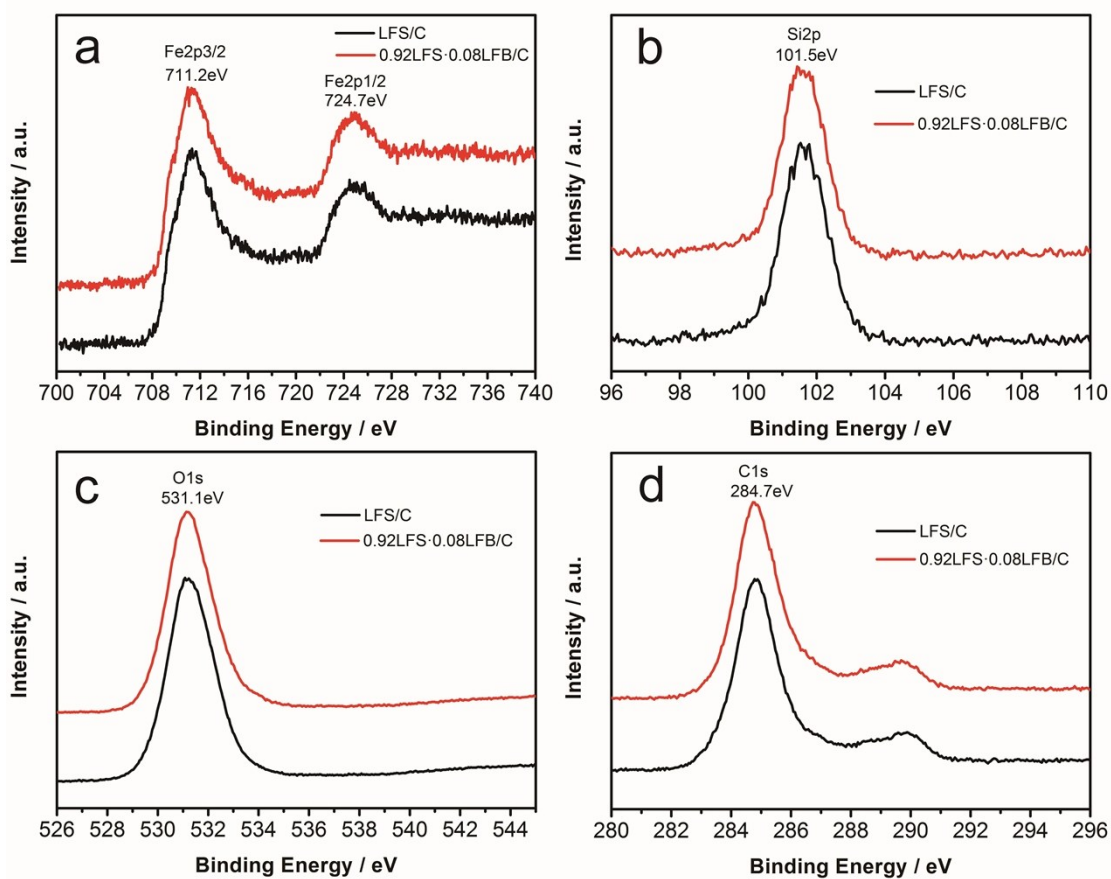
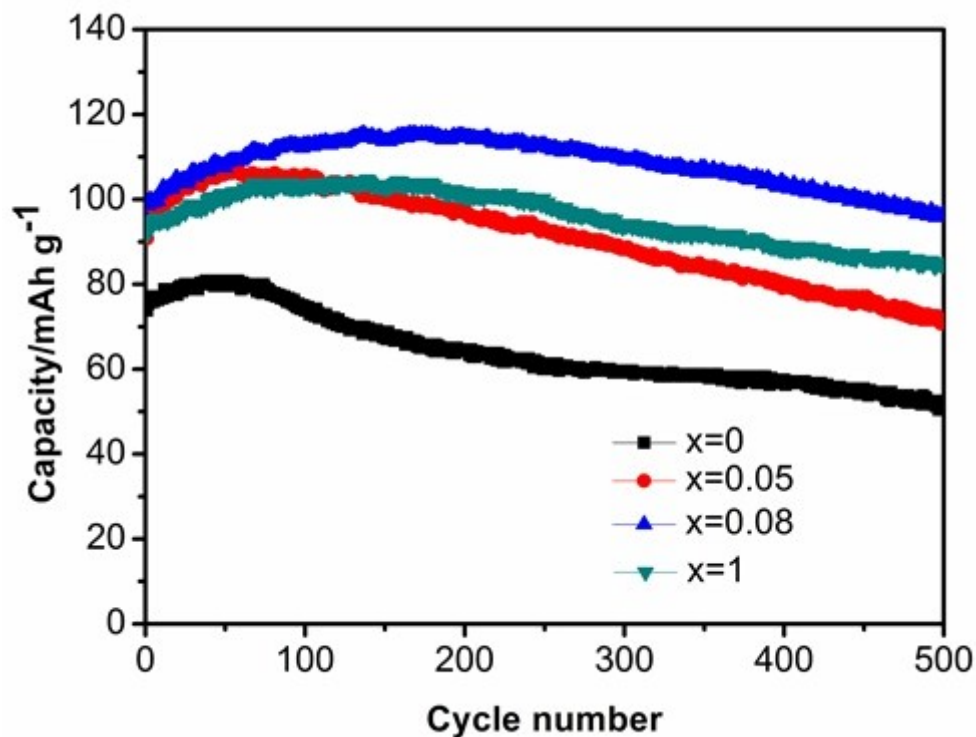**Figure S4.** SEM images of (1-x)LFS·xLFB/C composites with x=0.02 (a), 0.05 (b), 0.12 (c) and 1 (d).

Figure S5. TEM images of the LFS/C (a) and 0.92LFS·0.08LFB/C (b).
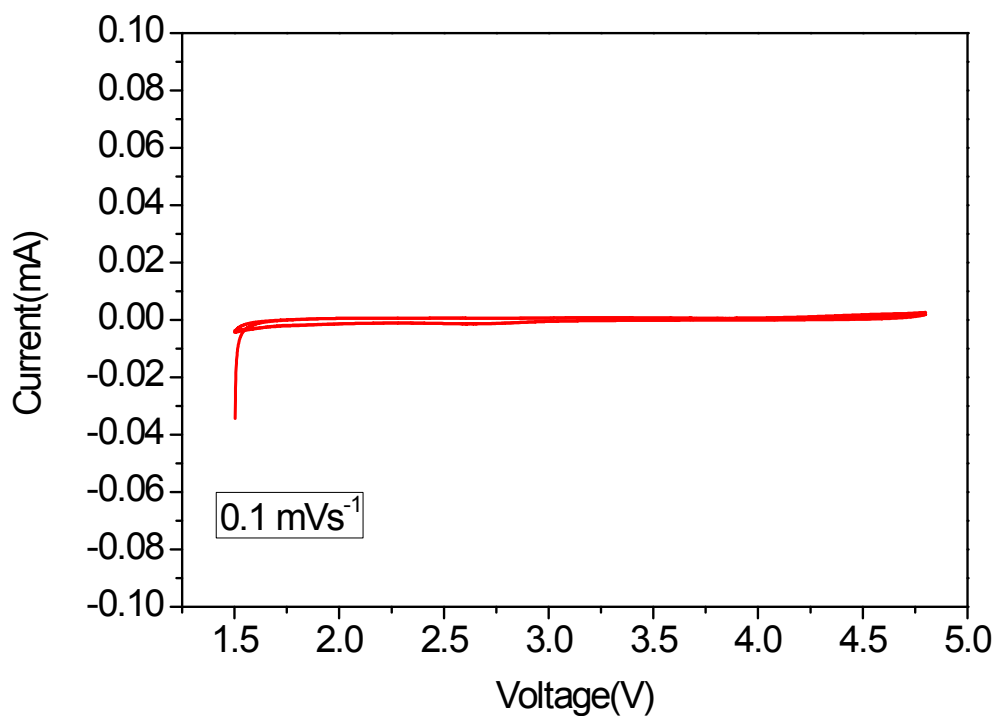
Figure S6.   XPS of -Fe2p (a), -Si2p (b), -O1s (c) and -C1s (d) spectrum of the LFS/C and 0.92LFS·0.08LFB/C samples.

Figure S7. Cycle performance of (1-x)LFS·xLFB/C samples at 10 C.

Figure S8 CV curves for the battery without a cathode at a rate of 0.1 mVs^{-1}.

Table S1 Data of the key elements content of the 0.92LFS·0.08LFB/C sample determined by the ICP analyses.

	Fe	Li	B
wt%	30.89	7.586	1.124
at%	0.553	1.093	0.104

EIS analyses

Figure 9a in text displays the Nyquist plots of LFS/C, 0.92LFS·0.08LFB/C and LFB/C electrodes. The high-frequency intercept on the real axis indicates the ohmic resistance (R_Ω) of total resistances including electrolyte, separator and electrical

contacts. The arc in the high-frequency region is related to the migration resistance (R_{SEI}) of lithium ions through the solid electrolyte interface (SEI), while the intermediate-frequency arc is attributed to the charge transfer resistance (R_{ct}) in the cathode-electrolyte interface. Both arcs are associated with the interface between electrolyte and active particles [1].

The constant phase element (CPE) replaces the conventional double-layer and passivation film capacitance [2]. The impedance of CPE is defined as:

$$Z_{CPE} = 1/(Y_0*(j\omega)^n) \qquad (1)$$

where ω is the angular frequency, j is imaginary unit, and Y_0 and n are constants. A CPE represents a resistor when $n = 0$, a Warburg resistance when $n = 0.5$, and a capacitor when $n = 1$.

The diffusion coefficient of lithium ions (D_{Li}) can be obtained according to the following equations [1, 3]:

$$D_{Li} = R^2T^2/2A^2n^4F^4C_{Li}^2\delta^2 \qquad (2)$$

where R is the gas constant, T is the absolute temperature, A is the surface area of the cathode, n is the number of electrons per molecule during oxidation, F is the Faraday constant, C_{Li} is the concentration of lithium ion, and δ is the Warburg coefficient which is related to Z' according to equation 3 [1, 3]:

$$Z' = (R_\Omega + R_{ct}) + \delta\omega^{-1/2} \qquad (3)$$

where ω is the angular frequency in the low frequency region, both R_Ω and R_{ct} are kinetics parameters independent of frequency, δ is the slope for the plot of Z' versus the reciprocal square root of the lower angular frequencies ($\omega^{-1/2}$). The Warburg

coefficient (δ) is obtained by linear fitting of Z′ versus $\omega^{-1/2}$ as shown in **Figure 9b** in text.

Table S2 The EIS parameters and diffusion coefficient of lithium ion for the LFS/C, 0.92LFS·0.08LFB/C and LFB/C samples tested at 45℃.

		LFS/C	0.92LFS·0.08LFB/C	LFB/C
Resistance (Ω)	R_Ω	4.7	17.6	5.1
	R_{SEI}	118.5	125.5	88.0
	R_{ct}	329.4	235.6	122.4
CPE_1 (S s^n)		3.01×10^{-5}	1.95×10^{-5}	6.47×10^{-5}
n_1		0.69	0.70	0.69
CPE_1 (S s^n)		2.51×10^{-4}	1.32×10^{-4}	8.94×10^{-5}
n_2		0.73	0.59	0.92
Z_w (S $s^{0.5}$)		7.42×10^{-3}	7.74×10^{-3}	1.15×10^{-2}
D ($cm^2 s^{-1}$)		2.36×10^{-14}	3.88×10^{-14}	1.14×10^{-13}

References

[1] R. Fu, Y. Li, H. Yang, Y. Zhang and X. Cheng, *Journal of The Electrochemical Society*, 2013, **160**, A3048-A3053.

[2] M. Ciureanu and R. Roberge, *The Journal of Physical Chemistry B*, 2001, **105**, 3531-3539.

[3] J. Yang, X. Kang, L. Hu, X. Gong and S. Mu, *Journal of Materials Chemistry A*, 2014, **2**, 6870-6878.